Pergamon

Ann. occup. Hyg., Vol. 40, No. 5, pp. 511–523, 1996

Published by Elsevier Science Ltd. Printed in Great Britain
0003–4878/96 $15.00 + 0.00

PII: S0003–4878(96)00003–8

THE EFFECT OF CONTAMINANT SOURCE LOCATION ON WORKER EXPOSURE IN THE NEAR-WAKE REGION

Ilpo Kulmala,*† Arto Säämänen‡ and Seppo Enbom‡

*Tampere University of Technology, Energy and Process Engineering, P.O. Box 589, FIN-33101 Tampere, Finland; and ‡VTT Manufacturing Technology, Safety Engineering, P.O. Box 1701, FIN-33101 Tampere, Finland

(*Received in final form* 16 *November* 1995)

Abstract—The exposure of workers in the near-wake region due to a recirculating airflow was studied experimentally and numerically. A mannequin was installed in an open-ended tunnel and tracer gas was released at several locations downstream to determine the size and location of the reverse flow region. The contaminant transport into the breathing zone was found to depend strongly on the location of the release point. The airflow field was also determined numerically assuming a steady flow and using the standard k–ε turbulence model. After calculating the turbulent airflow field, a large number of submicrometre particles were released in different locations downstream of the mannequin to simulate the transport of gaseous contaminants. Although this method does not provide actual exposures, it does predict the tendencies in exposure variations due to different release points quite satisfactorily. Copyright © 1996 British Occupational Hygiene Society.

NOMENCLATURE

C_μ	empirical constant in the k–ε turbulence model
H	tunnel height
h	height of mannequin
I	turbulence intensity
k	turbulence kinetic energy
P	mean pressure
U_i	mean velocity component in direction x_i
u_i	fluctuating velocity component in direction x_i
x_i	Cartesian co-ordinate in tensor notation
z	height
δ_{ij}	Kronecker delta, $\delta_{ij}=1$ for $i=j$ and 0 otherwise
ε	turbulence dissipation rate
ν	kinematic viscosity
ν_t	turbulent viscosity, $C_\mu k^2/\varepsilon$
ρ	fluid density

INTRODUCTION

In industry there are several operations where a horizontal unidirectional airflow is used to control airborne contaminants (George *et al.*, 1990; Andersson *et al.*, 1993; Guffey and Barnea, 1994). This kind of ventilation is also used in some non-industrial applications, such as indoor firing ranges. When a person is in a unidirectional airflow, however, a region with a recirculating airflow can be created

†Present address: VTT Manufacturing Technology, Safety Engineering, P.O. Box 1701, FIN-33101 Tampere, Finland.

downstream. Recent studies have shown that if the contaminant source and the breathing zone are within this near-wake region, high exposure may occur (Flynn and Ljungqvist, 1995).

When fluid flows past a blunt obstacle at a sufficiently high velocity, the flow separates from the body surface forming a wake region downstream of the obstacle. This wake region is frequently associated with periodic vortex shedding. There are several studies concerning the development of such wakes for some typical cases, such as two-dimensional circular and square cylinders (Cantwell and Coles, 1983; Franke and Rodi, 1991), and cubes (Robins and Castro, 1977; Larousse *et al.*, 1991; Murakami *et al.*, 1991).

Although the flow past simple geometries have been widely investigated, there are few numerical and experimental studies concerning the airflow around the worker. Flynn and Miller (1991) determined the flow field around the worker by solving numerically the unsteady Navier–Stokes equations using the discrete vortex method. Ingham and Yuan (1992) determined the flow past the worker into a line sink in a wall with the boundary element method. Recently, Dunnett (1994) predicted the time-dependent flow field using the k–ε turbulence model and artificial small perturbations to start the shedding process around the worker. In all these studies a two-dimensional flow was assumed and the worker was modelled as an ellipse.

It has been suggested that the transport of contaminants into and out of the near-wake zone of two-dimensional bodies is controlled primarily by vortex formation and shedding (MacLennan and Vincent, 1982). This approach was also used by George *et al.* (1990), who developed a simple model to determine the worker's breathing zone concentration. Recently, Flynn *et al.* (1995) used a particle trajectory method to predict the worker's exposure assuming a two-dimensional flow. Experiments have shown that the flow around the worker in a uniform airflow is three-dimensional (Kim and Flynn, 1991a) however, and therefore the airflow in the wake region may not be adequately described with two-dimensional models.

Previous investigations have studied the exposure when the contaminant source was fixed or the distance varied at the height of the chest only (Ljungqvist, 1979; George *et al.*, 1990; Kim and Flynn, 1991b). In this study the effect of the contaminant source location on exposure was examined more thoroughly when the source location was varied within the near-wake region. Extensive wind-tunnel measurements were made to study this phenomenon. In addition, numerical modelling was applied to the solving of the flow around the worker in a unidirectional airflow. The three-dimensional steady airflow field was calculated using the standard k–ε turbulence model. After calculating the airflow field, the variations in the worker's relative exposure to a contaminant source in the near-wake region were predicted by a particle tracking method, and the results were then compared with the measurements.

EXPERIMENTAL METHODS

The experiments were carried out in a tunnel 2 m high × 2 m wide × 4.2 m deep (Fig. 1). During the measurements the air was flowing freely in the tunnel from the surrounding laboratory room. The rear wall of the tunnel was fitted with a perforated plenum in order to get better air distribution across the tunnel. The

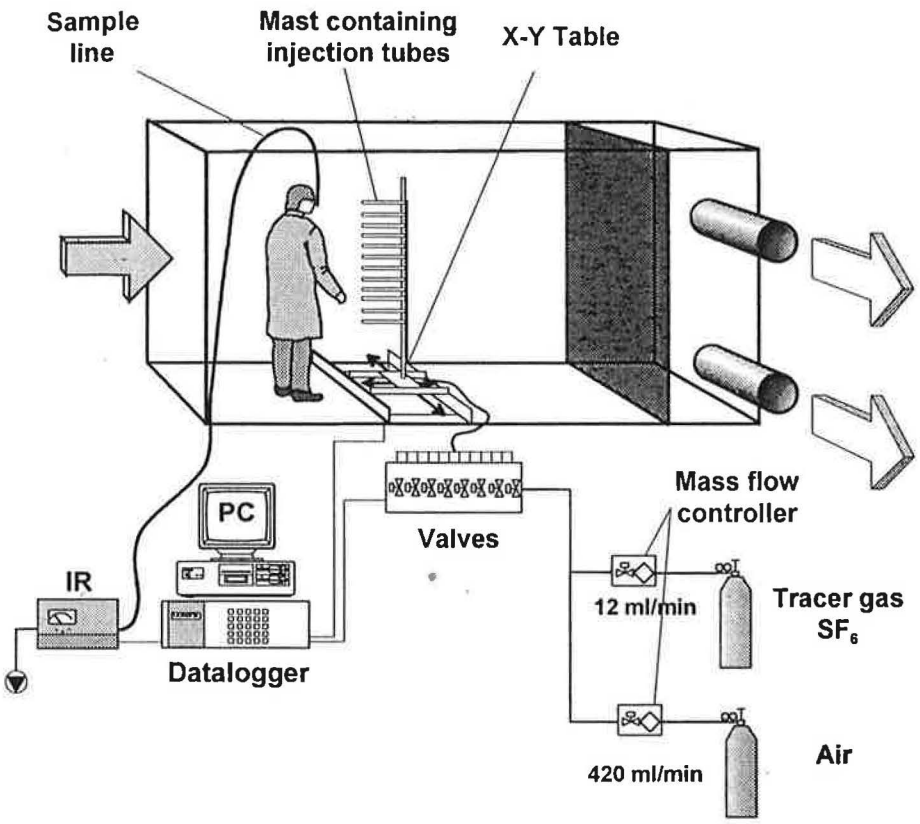

Fig. 1. Measurement system.

exhaust air was blown outside the building and the airflow rates were regulated by controlling the speed of the fan. An anthropometric mannequin, 1.52 m tall and 0.38 m wide at the shoulder, was facing downstream on the centreline of the tunnel about 0.85 m from the tunnel face. The experiments were carried out using mean freestream velocities of 0.25, 0.375 and 0.5 m s^{-1} (exhaust airflow rates of 1.0, 1.5 and 2.0 m^3 s^{-1}) corresponding to Reynolds numbers of 6300, 9500 and 12 700, respectively. The average turbulence intensity defined as the rms value of longitudinal velocity fluctuations to the mean longitudinal velocity of the empty tunnel was 32% measured at the location of the mannequin.

The effect of the contaminant source location on the worker's breathing zone concentration was examined by injecting tracer gas in several points downstream of the mannequin. Tracer gas was released from 420 points within the wake region. In the vertical direction the tracer gas injection was done by using 12 tubes in a mast with the lowest release point at 0.5 m and the highest point at 1.6 m height from the floor. A point source of contaminant was modelled so that the tracer gas discharged through 6 mm inside-diameter tubes directed towards the mannequin. The tracer gas jet exit velocities were about 0.25 m s^{-1}, and in order to study the effect of the jet momentum on the results the measurements were repeated at two distances (20 and

50 cm downstream of the mannequin) by using an almost momentumless source. This was done by releasing the tracer gas through porous cylindrical diffusers with a diameter of 15 mm and a length of 23 mm. Tracer gas was released from one tube at a time. The nearest release points were 0.2 m from the mannequin and the farthest points were 0.6 m downstream the body. The release points in the horizontal direction were spaced at 0.1 m intervals. In the lateral direction release points ranged from +0.3 to −0.3 m from the centreline at 0.1 m spacing. The mast containing tracer gas injection tubes was transferred both in horizontal and lateral directions using a computer-controlled X–Y table. The tracer gas, sulphur hexafluoride, was diluted to a 2.8% mixture with air. The air–SF_6 mixture was released with a flow rate of 432 ml min^{-1} using mass flow controllers (Bronkhorst Hi-Tech B.V., The Netherlands) to regulate the flow.

The breathing zone concentration of the tracer gas was sampled with a 10 mm dia. tube attached to the middle of the mannequin's nose and mouth (height 1.4 m). The sampling air flow rate was 20 l. min^{-1} and two infra red (i.r.) spectrophotometers, one for the concentration range 2–30 ppm (BINOS, Leybold & Heraeus Gmbh, Germany) and the other for the range 0.05–2 ppm (Miran 1A, Wilks Corporation, U.S.A.), were used to detect the sulphur hexafluoride concentration. The voltage signals from the i.r. analysers were sampled at the rate of 1 Hz for 100 s using a data logger (HP3497, Hewlett-Packard, U.S.A.) and a microcomputer. The mean values were computed from signals providing an estimate of the time-averaged concentration. The system was allowed to stabilize for 100 s before the sampling was started in each sampling point. Every freestream velocity was tested twice and the averages of the concentrations were calculated.

NUMERICAL SIMULATIONS

In the simulations, the flow field was solved assuming steady and isothermal flow. The time-averaged continuity and momentum equations can thus be written in tensor notation as

$$\frac{\partial U_i}{\partial x_i} = 0 \tag{1}$$

$$U_j \frac{\partial U_i}{\partial x_j} = -\frac{1}{\rho}\frac{\partial P}{\partial x_i} + \frac{\partial}{\partial x_j}\nu\left(\frac{\partial U_i}{\partial x_j} + \frac{\partial U_j}{\partial x_i}\right) - \frac{\partial}{\partial x_j}(\overline{u_i u_j}), \tag{2}$$

where U_i is the mean and u_i the fluctuating velocity component in the direction x_i, P is the mean pressure, ν is the kinematic viscosity and ρ is the fluid density. The study employed the standard k–ε turbulence model in which the Reynolds stresses are determined by using the Boussinesq approximation

$$-\overline{u_i u_j} = \nu\left(\frac{\partial U_i}{\partial x_j} + \frac{\partial U_j}{\partial x_i}\right) - \frac{2}{3}\delta_{ij}k, \tag{3}$$

where δ_{ij} is the Kronecker delta. The local turbulence viscosity ν_t is related to the kinetic energy of turbulence k and the dissipation rate of kinetic energy ε by the equation

$$\nu_t = C_\mu \frac{k^2}{\varepsilon}, \tag{4}$$

where C_μ is an empirical (usually $C_\mu = 0.09$). When determining a flow field, the modelled transport equations for k and ε are solved with the continuity and momentum equations. In the k–ε model it is assumed that the turbulent viscosity is isotropic so that the diffusion is independent of orientation relative to the flow direction. This assumption may cause inaccurate results in strongly anisotropic flows or flow regions.

The computational domain and the calculation grid are shown in Fig. 2. A vertical symmetry plane in the centreline was introduced to reduce the number of grid points. The mannequin was modelled with rectangular cells. Inhaling was modelled with an exhaust from the head at half the sampling flow rate (10 l. min^{-1}) because of the assumption of symmetry. The calculations were performed with two non-uniform grids of $41 \times 11 \times 29$ and $41 \times 20 \times 29$ points to study the effect of the grid refinement on the results. The mean-flow field was solved with a finite-volume based FLUENT version 3.02 computer code. A uniform velocity was assumed at the rear end of the tunnel and a fixed pressure at the tunnel face. The turbulent kinetic energy at the entrance was estimated by

$$k = \frac{1}{2}(\overline{u^2} + \overline{v^2} + \overline{w^2}) = \frac{3}{2}(IU_0)^2, \tag{5}$$

where I is the turbulence intensity (32%) and U_0 the mean freestream velocity. The inlet value of the dissipation rate was calculated by

$$\varepsilon = C_\mu^{3/4} \frac{k^{3/2}}{0.03H}, \tag{6}$$

where H is the height of the tunnel.

The shear stress at the mesh points closest to the walls and solid surfaces was obtained from logarithmic wall functions (Launder and Spalding, 1974). The

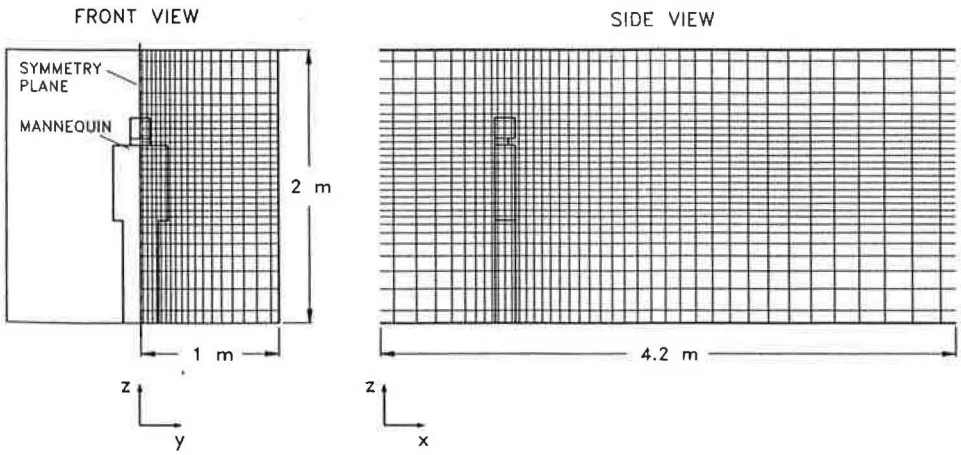

Fig. 2. Calculation domain and grid.

coupling between the continuity and momentum equations was achieved with th SIMPLE algorithm. The discretization scheme was QUICK. A solution for the flo field with the finer grid required about 600 min CPU time on a Sun Spark Server 69 MP. Sufficient convergence was assumed to be reached, when the sum of successiv fractional changes (residuals) was less than 10^{-3}.

After solving the flow field, the transport of airborne contaminants towards th worker's breathing zone was predicted by particle tracking, assuming that submicro particles are transported in the same way as gaseous contaminants (Kulmala, 1995) The dispersion of the particles around the mean flow streamlines due to turbulen fluctuations was obtained by assuming that the fluctuating velocity components obe the Gaussian probability distribution with the variance depending on the loca kinetic energy of turbulence. When a large number of particles were released in th near-wake region, some were captured by the exhaust in the head region, whicl simulated inhaling. Others were entrained in the tunnel exhaust. The calculation used the same release points as the experiments. The flight time of the particles fron the release point into the head sampling depended on the location of the release poin and it was 5–26 s. For a spherical particle with a diameter of 0.1 μm and with density of 1000 kg m^{-3} used in the calculations the relaxation time is abou 8.8×10^{-8} s. Therefore, small particles will adjust almost instantly to the air velocit and they follow the turbulent fluctuations accurately. The highest particle counts a the freestream velocity of 0.375 m s^{-1} were observed when the release point was i the centreline at a height of 1.2 m and 0.2 m downstream of the mannequin. This wa taken to be the reference particle count value. The relative breathing zone particl count at different release points was then calculated as the ratio of particles entraine in the sampling in the head compared to the reference particle count. This metho does not give contaminant concentrations and therefore the worker's actua exposure cannot be predicted. The particle tracking method is valuable in estimatin the changes in the breathing zone concentrations, however, due to spatially varyin release points and also in predicting the efficiency of possible control measures. Th estimates of the worker's relative exposure were based upon 1000 particle paths fron each release point. The calculations were also repeated in some cases with 10 00 release particles but no significant differences between the results were found. Th tracking of 1000 particles took about 3 min of CPU time.

RESULTS

The concentration contours in Fig. 3 show the measured breathing zon concentrations due to different release points in the vertical sections 10 cm to the lef of the mid-plane, on the mid-plane and 10 cm to the right of the mid-plane. These results were normalized by dividing the measured concentrations by the highes concentration observed when the exhaust airflow rate was 1.5 m^3 s^{-1}. This maximum concentration (10.8 ppm) occurred when the release point was on the mid-plane 20 cm from the mannequin at a height of 1.2 m. The contours are for a tunne airflow rate of 1.5 m^3 s^{-1} but the same kind of results were obtained with othe exhaust flow rates. It can be seen that the breathing zone concentration depends on the height and the distance of the contaminant source from the body and as on the distance from the vertical mid-section. The exposure decreases rapidly when the

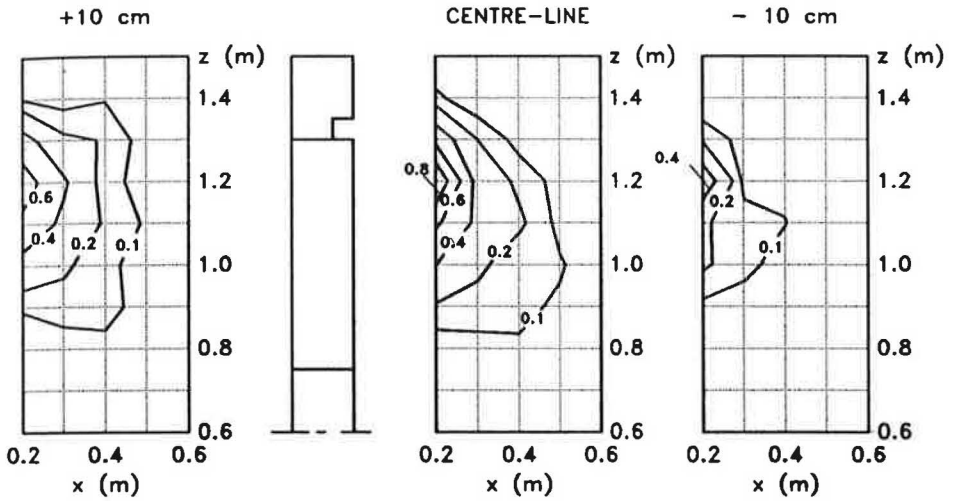

Fig. 3. Measured relative exposure in the vertical sections due to tracer gas release with a mean freestream velocity of 0.375 m s^{-1}.

distance between the worker's body and the contaminant source increases. As the air flows over the mannequin's head, there is a separation, and the flow is deflected downwards. This downwash means that little contamination released above this shear layer is transported into the breathing zone. The lack of symmetry in the results was also found with the other freestream velocities and it probably reflects the spatial variations in the flow field and the asymmetry of the mannequin.

The concentration profiles with the bare tracer gas injection tube and with the momentumless source (diffusor) are compared in Fig. 4. The results are averages of five repetitions. There were some differences in the concentrations but they were not statistically significant, except for two release points at lower heights (60 and 70 cm 0.5 m downstream of the mannequin). These release points had little effect on the exposure, however, therefore it can be concluded that the momentum of the tracer gas, which was released through the tubes, had a negligible effect on the results.

The measured relative breathing zone concentrations and the calculated particle counts in the vertical mid-plane are compared in Fig. 5. These results are also normalized using the same reference concentration with the airflow of 1.5 m^3 s^{-1} as in Fig. 3. Considering the experimental scatter in the measurements and asymmetry of the flow the overall agreement in the trends between the predictions and the experiments was quite good. The height and length of the recirculating region was well predicted. Moreover, the location of the contaminant release point producing the highest concentration was correctly predicted. The length of the region, where significant contaminant transport occurs into the breathing zone (over 10% of the reference concentration), was about 0.5–0.6 m and it was not much affected by the freestream velocity.

The calculated mean velocity vectors and U-velocity profiles with the average freestream velocity of 0.375 m s^{-1} are shown in Fig. 6. This flow pattern is also in good agreement with the visual observations reported by Kim and Flynn (1991a). The predicted regions causing 10 and 80% of the reference particle count value are

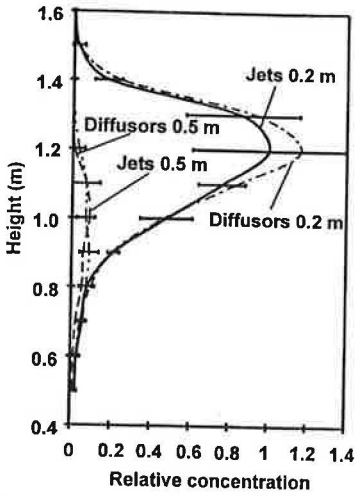

Fig. 4. Measured relative breathing zone concentration profiles with momentumless source (diffusors) and with jet. The horizontal bars indicate 95% confidence interval. The freestream velocity was 0.375 m s^{-1}.

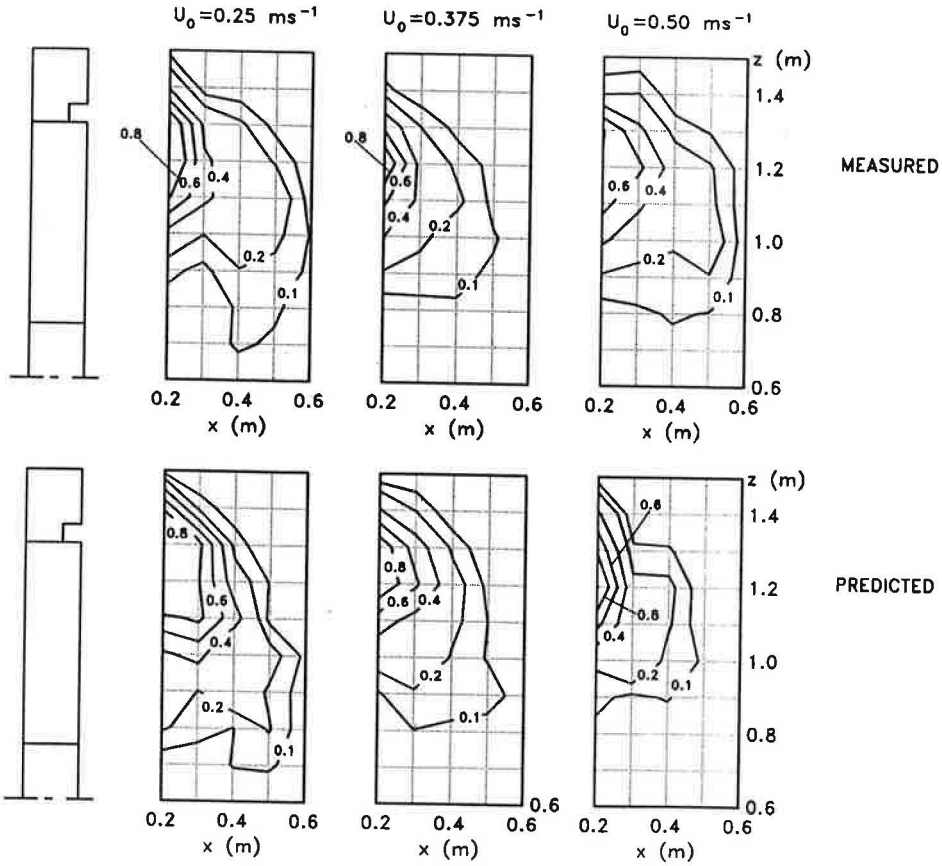

Fig. 5. Measured relative exposures and predicted relative particle counts in the vertical mid-plane with various mean freestream velocities.

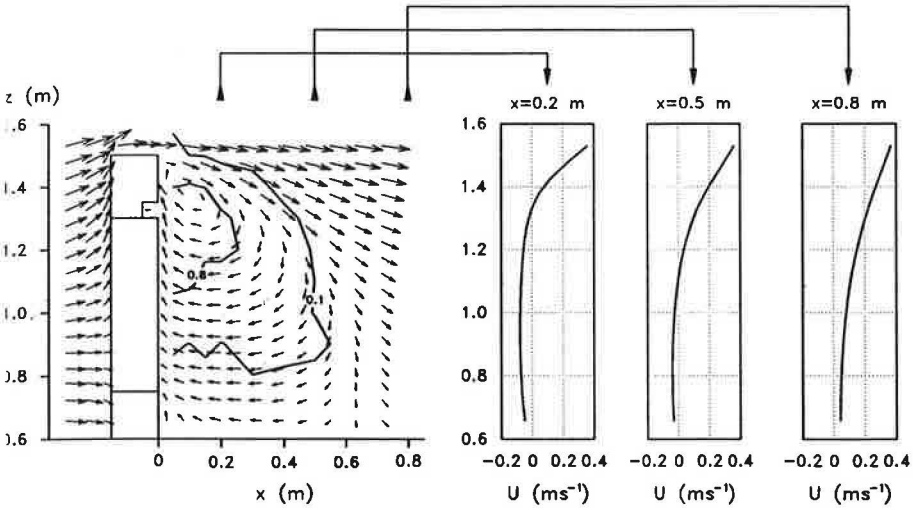

g. 6. Predicted mean flow field and velocity profiles downstream of the mannequin in the vertical mid-section.

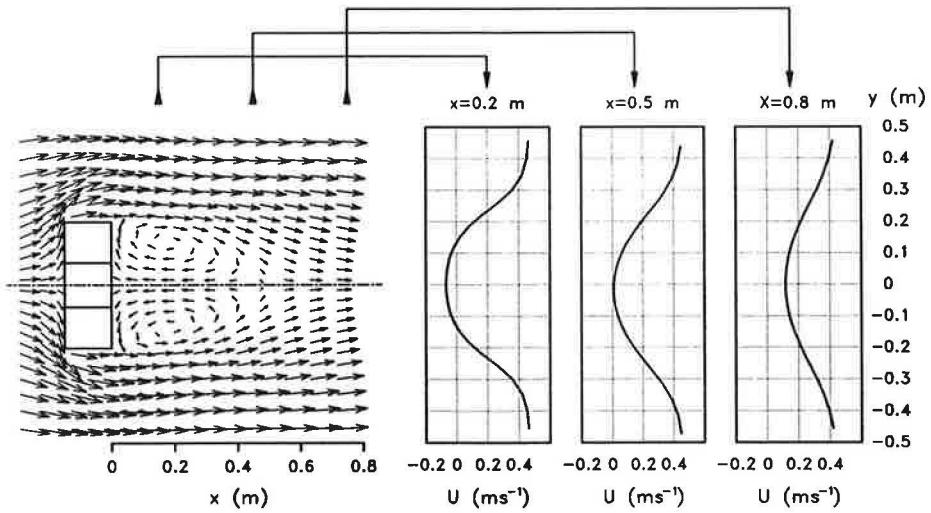

g. 7. Predicted mean flow field and velocity profiles downstream of the mannequin in a horizontal plane. The velocities have been reflected in the plane of symmetry.

so overlaid in the figure. Figure 7 shows the mean velocity vectors projected onto a orizontal plane at a height of 1.1 m parallel to the main flow direction. From these gures the flow pattern in the reverse flow region can be clearly seen. For clarity, the ngth of the velocity vectors is proportional to the square root of the velocity agnitude. These mean air velocity fields also help us to understand the contaminant ansport into the breathing zone and to explain the measured exposures. In the ertical section approximately above the mannequin's hip level ($z > 0.8$ m, Fig. 6) the r circulates clockwise and contaminants released in this region may enter the

breathing zone. On the other hand, below the hip level the air circulates mainly horizontally and the contaminants released in this region do not significantly enter the breathing zone.

An increase in the grid density did not greatly affect the predicted velocities, although the recirculation length was higher with the coarser grid. It is difficult to say whether grid-independent solutions were obtained because further refinements in the grid density were not possible due to the limitations of the computer resources.

The predicted mean velocities in the reverse flow were clearly lower than the freestream velocities. Maximum velocities towards the mannequin depended somewhat on the freestream velocity but were below 0.1 m s^{-1}. The predictions therefore suggest that the reverse flow momentum is so low that the worker's exposure could possibly be controlled by appropriate measures.

DISCUSSION

The aims of this study were to investigate the effect of the contaminant source location on the worker's exposure in the near-wake region and the applicability of numerically modelling this situation. The flow field downstream of the worker is very complex and the results revealed that the exposure depends greatly on the location of the contaminant source. Despite the deficiencies of the simulations these variations could be predicted quite well in the centreline assuming a steady flow. The contaminant source position which caused the greatest exposure was predicted surprisingly well, but asymmetry was found in the measured concentration fields contrary to the calculations where symmetry was assumed about the vertical mid-plane.

An important feature in the near-wake region is the size and location of the recirculation zone downstream of the worker because contaminants released in this region can enter the breathing zone. The mean recirculation length depended little on the freestream velocity and it appeared to be about 1.5 times the mannequin's width downstream of the body. The breathing zone concentration decreases rapidly when the distance of the contaminant source from the body increases. It was also observed that significant contaminant transport toward the breathing zone occurs only above the hip level ($z/h > 0.53$). These findings are in general agreement with previous studies (George *et al.*, 1990; Kim and Flynn, 1991a).

In the numerical model, the transport of contaminants into the breathing zone depends on the mean flow field as well as on the turbulent dispersion of the contaminants about the mean flow streamlines. This, in turn, depends on the local state of turbulence which in this model was characterized by the turbulent kinetic energy and its dissipation rate. Therefore, for accurate breathing zone concentration predictions both the mean velocity field and the turbulent kinetic energy should be correctly calculated.

The accuracy of numerical calculations usually depends on several components of the simulation method, such as the applicability of the adopted turbulence model, computation grid, reliability of the boundary conditions and the discretization scheme. In these calculations the factors having the greatest effect on the accuracy were the geometrical approximations, the presumption of symmetric and steady flow, and the shortcomings of the k–ε turbulence model.

The tracer gas measurements indicated asymmetry about the centreline although the measured maximum concentration levels were observed in the vertical mid-section. The mannequin's arms and body were also in a somewhat asymmetric position. In addition, the mannequin was approximated quite crudely by parallelepiped cells. The calculations also assumed symmetric velocity distribution about the centreline at the entrance but the air velocity measurements revealed that the velocity was non-uniform and somewhat asymmetric. The spatial variation of the velocities was 27%. This kind of variation is, however, quite common in industrial ventilation applications.

It is well known that the periodic vortex shedding frequency of flows past slender two-dimensional bodies is nearly constant for a wide range of Reynolds number. The frequency depends on the aspect ratio of the obstacle, however, so that the Strouhal number decreases with decreasing aspect ratio. In addition, it has been discovered (Sakamoto and Arie, 1983) that the level of fluctuating velocity caused by vortex shedding approaches the level of other irregular velocity fluctuations when the aspect ratio is less than 1.0 for square cylinders and less than 1.5 for circular cylinders, suggesting that the periodic vortex shedding disappears. Kim and Flynn (1991a) measured the shedding frequencies at different heights in the wake region of a mannequin and found that the prominent frequency peaks characterizing the vortex shedding frequency depended on the height. They found prominent frequency peaks between the waist and hip levels ($0.44 < z/h < 0.54$) but not above the elbow level ($z/h > 0.63$). It can be concluded, therefore, that the flow past a worker in uniform flow may be periodic in some regions. Steady-state calculations do not reveal this phenomenon and are probably erroneous in predicting the mean flow field in these regions since the strong momentum exchange by periodic vortex motion is not accounted for in this approach (Franke and Rodi, 1991). Nevertheless, the results proved that the most important region affecting the worker's exposure is between the waist and the head level and that the flow field in this region may be predicted reasonably well with steady flow calculations.

The k–ε model is currently perhaps the most commonly used turbulence model for practical calculations and it has been applied successfully to a wide range of flow predictions. Recent studies have indicated that the standard k–ε model may not predict the flow past bluff bodies very well (Obi *et al.*, 1990; Franke and Rodi, 1991; Murakami *et al.*, 1991), however, the inaccuracies are caused by the assumption of isotropic turbulent viscosity and gradient hypothesis for the Reynolds stresses. Better agreement with the measured flow fields were obtained with the Reynolds stress models, which take the turbulence anisotropy and flow history effects on the turbulence into account. Even these more sophisticated models were not fully satisfactory, however, and it was concluded that the most accurate results may be obtained using the large-eddy simulation (LES). In this approach the large eddies are computed and only the smallest eddies are modelled. The LES is considered to be a potentially promising method, but so far the very large computational resource requirements have limited its application to research topics. On the other hand, the differences between the geometry of the mannequin in reality and in the simulations, spatial variations of the flow velocities and possible periodicities of the flow may have greater effect on the results than the turbulence model.

It has been suggested (George *et al.*, 1990; Kim and Flynn, 1991a) that exposure can be estimated by assuming the flow to be two-dimensional and that the contaminant removal is primarily due to the vortex shedding. The results of this study show, however, that the flow is three-dimensional and that the exposure strongly depends on the distance between the contaminant source and the worker's body, as well as on the height and distance from the centreline. The measurements also show that the upper recirculation zone in the near wake is the most important region causing worker's exposure. Furthermore, the relatively good agreement between calculations and experiments implies that despite the imperfections of the computational method used and the complexity of the real flow the three-dimensional steady-state simulations can give useful results when predicting the flow field in this region.

Kim and Flynn (1992) studied the source momentum effect on the worker's exposure in a wind tunnel by releasing gas through jets directed outwards from the mannequin. They discovered that a source momentum as small as the momentum of jets used in this study caused a reduction in breathing zone concentrations. Contrary to their results, the effect of the source momentum in this study was not statistically significant. The data in their study do not permit a direct comparison, however, because the jet directions were different and the exact contaminant release point was not reported. The nearest release point in this study was 0.2 m from the mannequin, while in Kim and Flynn's study the source was probably located closer to the mannequin.

The results are applicable when a stationary worker is in a uniform airflow and the momentum of the contaminant source is negligible. These restrictions are rarely met under actual working conditions. However, the results are useful in understanding the transport of contaminants in the near-wake region. One of the advantages of numerical simulations is the possibility to study various effects on the exposure once a verified model has been developed. Research is under way to examine how to reduce the exposure effectively.

Acknowledgements—This work was financially supported by the Finnish Work Environment Fund (TSR) and Finnish Technology Development Centre (TEKES).

REFERENCES

Andersson, I.-M., Niemelä, R., Rosén, G. and Säämänen, A. (1993) Control of styrene exposure by horizontal displacement ventilation. *Appl. occup. Environ. Hyg.* **8,** 1031–1037.

Cantwell, B. and Coles, D. (1983) An experimental study of entrainment and transport in the turbulent near wake of a circular cylinder. *J. Fluid Mech.* **136,** 321–374.

Dunnett, S. J. (1994) A numerical investigation into the flow field around a worker positioned by an exhaust opening. *Ann. occup. Hyg.* **38,** 663–686.

Flynn, M. R., Chen, M-M., Kim, T. and Muthedath, P. (1995) Computational simulation of worker exposure using a particle trajectory method. *Ann. occup. Hyg.* **39,** 277–289.

Flynn, M. R. and Ljungqvist, B. (1995) A review of wake effects on worker exposure. *Ann. occup. Hyg.* **39,** 211–221.

Flynn, M. R. and Miller, C. T. (1991) Discrete vortex methods for the simulation of boundary layer separation effects on worker exposure. *Ann. occup. Hyg.* **35,** 35–50.

Franke, R. and Rodi, W. (1991) Calculation of vortex shedding past a square cylinder with various turbulence models. In *Proc. Eight Symposium on Turbulent Shear Flows*, Technical University of Munich, Germany, pp. 20.1.1–20.1.6.

George, D. K., Flynn, M. R. and Goodman, R. (1990) The impact of boundary layer separation on local exhaust design and worker exposure. *Appl. occup. Environ. Hyg.* **5,** 501–509.

Guffey, S. and Barnea, N. (1994) Effects of face velocity, flanges, and mannikin position on the effectiveness of a benchtop enclosing hood in the absence of cross-drafts. *Am. ind. Hyg. Ass. J.* **55,** 132–139.

Ingham, D. B. and Yuan, Y. (1992) A mathematical model for the air flow around a worker near a fume cupboard. *Ann. occup. Hyg.* **36,** 441–453.

Kim, T. and Flynn, M. R. (1991a) Airflow pattern around a worker in a uniform freestream. *Am. ind. Hyg. Ass. J.* **52,** 287–296.

Kim, T. and Flynn, M. R. (1991b) Modeling a worker's exposure from a hand-held source in a uniform freestream. *Am. ind. Hyg. Ass. J.* **52,** 458–463.

Kim, T. and Flynn, M. R. (1992) The effect of contaminant source momentum on a worker's breathing zone concentration in a uniform freestream. *Am. ind. Hyg. Ass. J.* **53,** 757–766.

Kulmala, I. (1995) Numerical simulation of the capture efficiency of an unflanged rectangular exhaust opening in a coaxial air flow field. *Ann. occup. Hyg.* **39,** 21–33.

Larousse, A., Martinuzzi, R. and Tropea, C. (1991) Flow around surface-mounted, three-dimensional obstacles. In *Proc. Eight Symposium on Turbulent Shear Flows*, pp. 14.4.1–14.4.6.

Launder, B. E. and Spalding, D. B. (1974) The numerical computation of turbulent flows. *Comput. Meth. appl. Mech. Engng* **3,** 269–289.

Ljungqvist, B. (1979) Some observations on the interaction between air movements and the dispersion of pollution. Document D8. Swedish Council for Building Research, Stockholm, Sweden.

MacLennan, A. S. and Vincent, J. H. (1982) Transport in the near aerodynamic wakes of flat plates. *J. Fluid Mech.* **120,** 185–197.

Murakami, S., Mochida, A. and Hayashi, Y. (1991) Scrutinizing k–ε evm and ASM by means of LES and wind tunnel for flow around cube. In *Proc. Eight Symposium on Turbulent Shear Flows*, pp. 17.1.1–17.1.6.

Obi, S., Perić, M. and Scheuerer, G. (1990) Finite volume computation of the flow over a square rib using a second order turbulence closure. In *Engineering Turbulence Modelling and Experiments* (Edited by Rodi, W. and Ganić, E.), pp. 185–194. Elsevier, New York.

Robins, A. G. and Castro, I. P. (1977) A wind tunnel investigation of plume dispersion in the vicinity of a surface mounted cube-I. The flow field. *Atmospheric Environment* **11,** 291–297.

Sakamoto, H. and Arie, M. (1983) Vortex shedding from a rectangular prism and a circular cylinder placed vertically in a turbulent boundary layer. *J. Fluid Mech.* **126,** 147–165.

Werner, H. and Wengle, H. (1991) Large eddy simulation of turbulent flow over and around a cube in a plate channel. In *Proc. Eight Symposium on Turbulent Shear Flows*, pp. 19.4.1–19.4.6.